VARIATION OF THE OBSERVED SURFACE STRAINS CAUSED BY UNIFORM AND NON-UNIFORM CONTACT PRESSURES USING A FINITE ELEMENT METHOD

D.B. Casey, G.D. Airey & J.R. Grenfell
Nottingham Transportation Engineering centre (NTEC), University of Nottingham, U.K.
Dermot.casey@nottingham.ac.uk, Gordon.airey@nottingham.ac.uk &
James.grenfell@nottingham.ac.uk
A.C. Collop
Faculty of Technology, De Montfort University, Leicester, U.K.
acollop@dmu.ac.uk

ABSTRACT

The current practice in pavement design is to use a circular uniformly distributed load as the input to ascertain the maximum strains in the pavement. This is not the reality; tyre-pavement contact pressure distributions are very complex. The distress on the surface of the pavement in the form of rutting and surface initiated cracking is very much dependent on these complex pressure distributions. This study investigates the effects that non-uniform contact pressure distributions have in comparison to the traditional circular loading on the initiation and rate of accumulation of this distress. The problem has been modelled using the CAPA-3D finite element software. The traditional circular load was modelled. The strains in a number of key locations were recorded and measured. Then the non-uniform loading was modelled using the same procedure. What was of particular interest was the difference in the peak surface strains and positions between the two different methods of loading. The non-uniform loading created significantly larger strains under the contact patch. The non-uniform loading also created significant shearing forces close to the surface and under the contact area. This leads to a greater propensity for the surface to develop rutting and also for cracking. The differences started to become less evident with distance from the loading area for the principal stresses. It is recommended that for the design of surface layers non-uniform contact pressures should be used.

1. INTRODUCTION

Tyre inflation pressure has increased significantly since the AASHO road tests of the 1960s [1]. There has also been an increase in the permitted axle loading. This has led to an increase in both the inflation pressure and axle load and a change in tyre type from bias ply tyres to radial ply tyres. This creates increased loads with higher inflation pressures on tyres with greater non-uniformity of pressure [2]. This added to the development of wide base tyres with smaller contact areas increases the problem further. It is believed that this leads to increased damage to the pavement and also premature pavement damage, especially at the surface. The trend in increased inflation pressures has been seen in a study by Morton [3]. The survey showed that from 1974-1995 the average inflation increased from 620kPa to 733kPa.

The current practice in pavement engineering is to use a circular uniform contact patch to represent a tyre load. This is used in conjunction with a Layered elastic program like BISAR to estimate the maximum tensile strain at the bottom of the asphalt layers and the maximum compressive strain at the top of the subgrade. However, this method was shown

to overestimate the tensile strain at the bottom of the asphalt layers and the compressive strain at the top of subgrade [4]. This study also looked at the effects of tyre pressures on pavement response; it was shown that increased tyre pressure can increase the propensity of the pavement to fatigue and rutting damage. De Beer has done a number of studies using the Vehicle-Road Surface Pressure Transducer Array (VRSPTA) to quantify the magnitude and range of contact pressure geometries in the vertical, lateral and longitudinal directions [5-8]. This has given a great insight in the true nature of contact pressures that pavements are subjected to. It has been shown that the reality of contact pressure is far removed from the idealised scenario of a uniform circular contact patch. The pressure is highly non-uniform with peaks of vertical pressure 1-2 times the inflation pressure (the inflation pressure is usually used to represent the contact pressure). The shape is predominately rectangular and the width is relatively constant over a range of inflation pressures and axle loads. The shape of the contact pressure is dependent on the combination of tyre type, inflation pressure and axle load. This makes the increase in the inflation pressure, axle load and change in tyre designs rather worrying.

The non-uniformity of contact pressure leads to high stresses and strains on and near the surface of the pavement. These stresses and strains are higher than those created at the bottom of the asphalt and the top of the subgrade. This then gives rise to premature distress and maintenance interventions and causes an increased economic cost to the infrastructure stakeholders. The phenomenon of top down cracking has been highlighted by many researchers [9-11]. The cause of this cracking has not been conclusively proven but tyre contact pressures are believed to be a leading factor in this behaviour [12]. The distress mode of surface rutting is also linked to the contact pressure being imposed on the pavement [13]. These two modes of distress are influenced by the type and magnitude of stresses and strains on and near the surface of the asphalt layer. The nature of the contact pressure influences both the size of the peak stresses and strains but also where they are observed e.g. inside or outside the contact area [14].

In this paper, the effects of non-uniform vertical contact pressure on pavement response were investigated using a linear elastic constitutive model in the CAPA-3D Finite element package. The pavement response was predicted for the near surface strains under the loading area and away from it. A uniform circular contact patch was applied and a rectangular contact patch with a simplified non-uniform contact pressure from De Beer's VRSPTA was applied to a Finite Element mesh. These two loads and two different asphalt moduli (one high, one low) were used to investigate the effect of non-uniform contact pressure.

1.1 Objectives

- To establish the variation in the strains induced on the surface and the near surface by non-uniform contact pressure in comparison with uniform contact pressure.
- To illustrate how the effects of the non-uniform contact pressure vary with depth and/or distance from the contact area.
- To highlighting the shear strains that the non-uniform contact pressure induce under the contact area.

2. PROCEDURE

2.1 Mesh Validation

Choosing the correct mesh geometry with proper boundary conditions is a critical element of the analysis. It is an area that has the largest input from the user and as such is prone to the most mistakes. The refinement of the mesh was a time consuming activity but is essential to balance the refinement of the mesh with the conflicting requirement of minimising the computational resources required. It was decided to create a complete model with no axes of symmetry present due to the nature of non-uniform contact pressures. The method of validating the mesh was to compare the stress and strain outputs at specific locations with that of BISAR for the uniform circular loading. BISAR is a well used layered elastic program that has been validated numerous times and represents an excellent benchmarking tool for the Finite Element model. The output from the near surface and under the loading was of particular interest and was used for the validating procedure.

The mesh that is presented in Figure 1 is the mesh that was chosen from the analysis of various mesh geometries and boundary conditions. It represents a good mix between accuracy of stresses in the analysis area and reasonable running times. The base of the mesh is fixed in the x, y and z planes, and the four sides of the model are restrained in the horizontal direction. The overall dimension of the model of 4m by 4m in the x and z planes and 2.45m in the y plane was chosen to make the end effects of the boundary conditions negligible to the analysis. The layers are made up of a 0.15m asphalt layer on a 0.3m subbase layer on top of 2m of subgrade material measured in the Y axis.

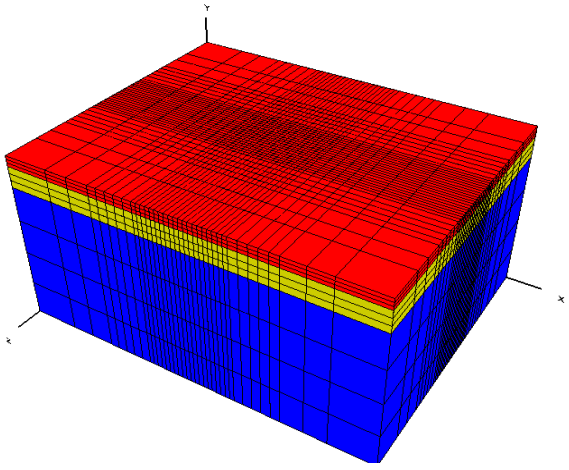

Figure 1 - Model with the selected mesh refinement

Stress and strain outputs at a depth of 2.5mm and 27.5mm compared well with that of BISAR. The Finite Elements solution slightly underestimated the stresses and strains which is common for the Finite Element Method. This is an acceptable error as it is expected and only represents a small variation and will be constant in both the uniform and non-uniform analysis. The material properties of the model are shown in Table I. The

base modulus is on the high side as it is the purpose of this study to investigate the strains in the asphalt layer.

Table 1 – Model Material Properties

	Young's Modulus (MPa)	*Poisson Ratio*
Asphalt	4500	0.35
Base	700	0.35
Subgrade	100	0.35

2.2 Selection of Loading

The loading of the circular contact patch was chosen as 150mm radius with a uniform vertical loading of 666kPa. This is a common representation of a tyre loading both in terms of contact pressure and the area of loading. This is also approximately the area of the non-uniform contact patch which lends itself to a good comparison. The loading was chosen as it is a common contact pressure and will show the strains created by this loading scenario. The non-uniform contact pressure is a rectangle of 240mm wide by 285mm long for a 315/80R22.5 tyre that is commonly used on the steering axle. The measurements of the tyre contact pressure were obtained from De Beer's VRSPTA. The author has divided the pressure into 9 regions of constant contact pressure based on the distribution of the readings. The width is divided into 20% 60% 20% ratios, as is the length. The readings in these areas are summed and averaged to obtain the reading for that region. This gives a good estimation of the nature of the contact pressure of the tyre. The magnitude of the loading on these regions can be seen in Figure 2.

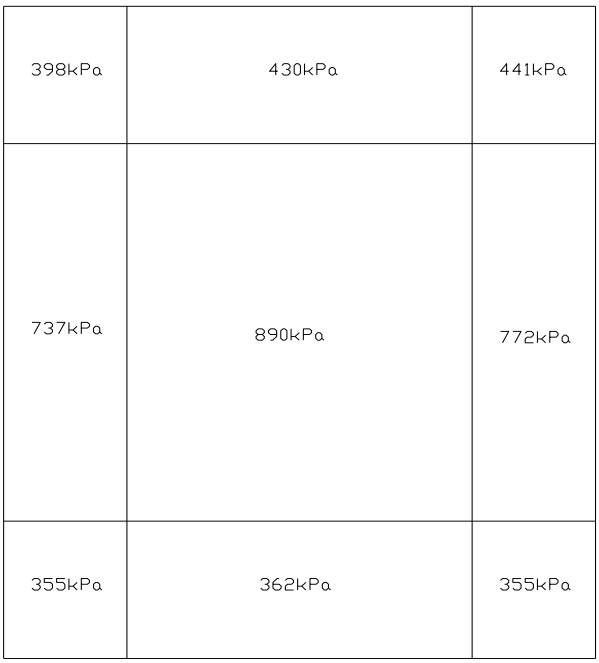

Figure 2 - Map of the non-uniform contact patch

2.3 Output Positions

CAPA-3D gives text stress and strain output at the integration points in the elements. These points are the positions where these outputs are most accurate and as such these are the points that were used for visualising the output from each analysis. The purpose of this paper is to compare the near surface strains; therefore, the upper most elements were used. These points are at a depth of 2.5mm, then to observe the effect depth has on the output; points at 27.5mm were also represented. The cross section has been taken underneath the loaded area moving out along the x plane to a distance of 500mm from the centre of loading. A close up of this area of the mesh can be seen in Figure 3.

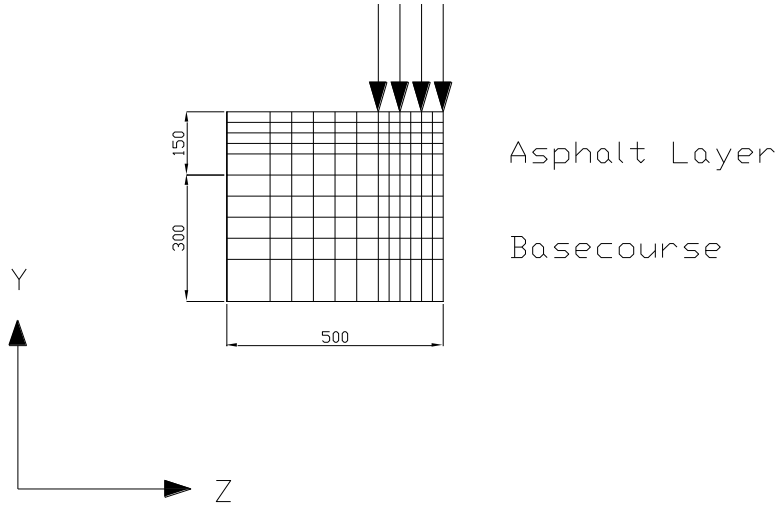

Figure 3 - Close-up of the area of interest for analysis

This area will be used to show the differences in all the loading scenarios.

3 RESULTS AND DISSCUSSION

3.1 NEAR SURFACE STRAINS

The graphs presented in Figure 4 are showing the principal strains that were recorded for the analysis at a 2.5mm depth. The graphs compare the two loading scenarios of uniform and non-uniform contact pressures to illustrate the different strain profiles that are created. These show quite clearly how much of an influence the contact pressure distribution has on the strain response at this depth.

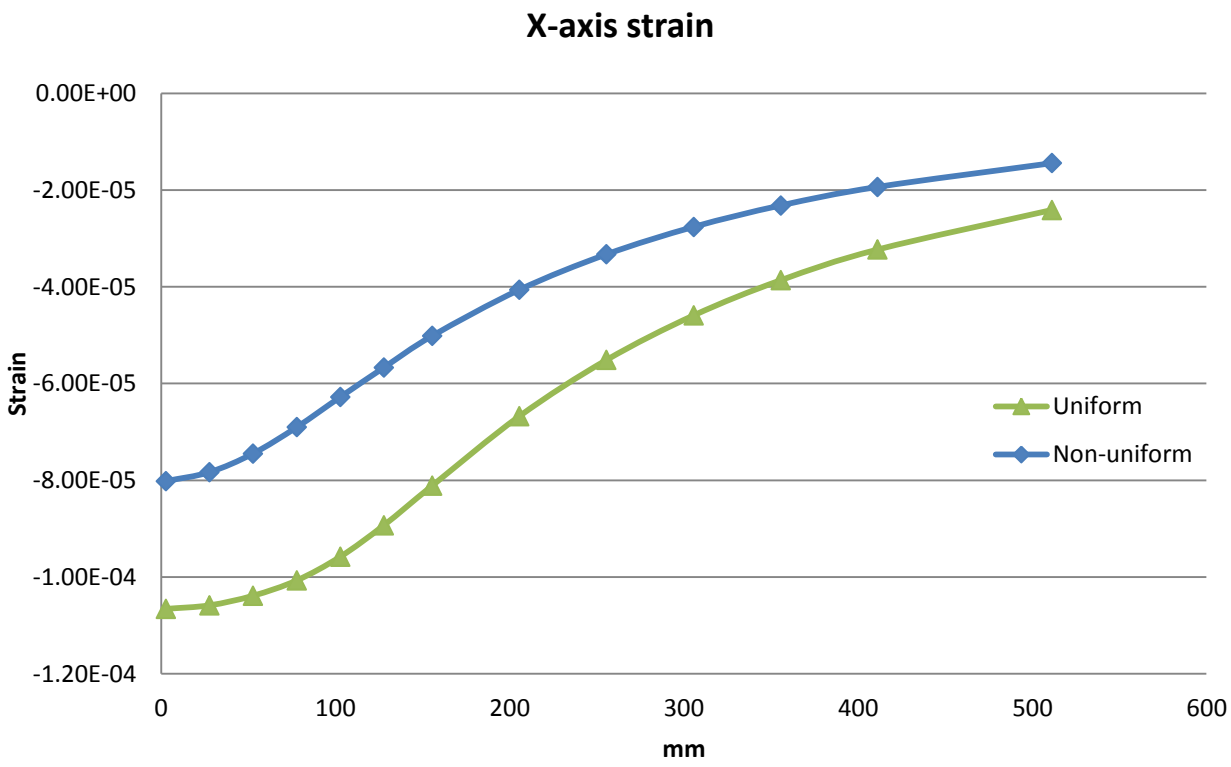
X-axis strain
0.00E+00
-2.00E-05
-4.00E-05
-6.00E-05
-8.00E-05
-1.00E-04
-1.20E-04
Strain
0
100
200
300
400
500
600
mm
Uniform
Non-uniform

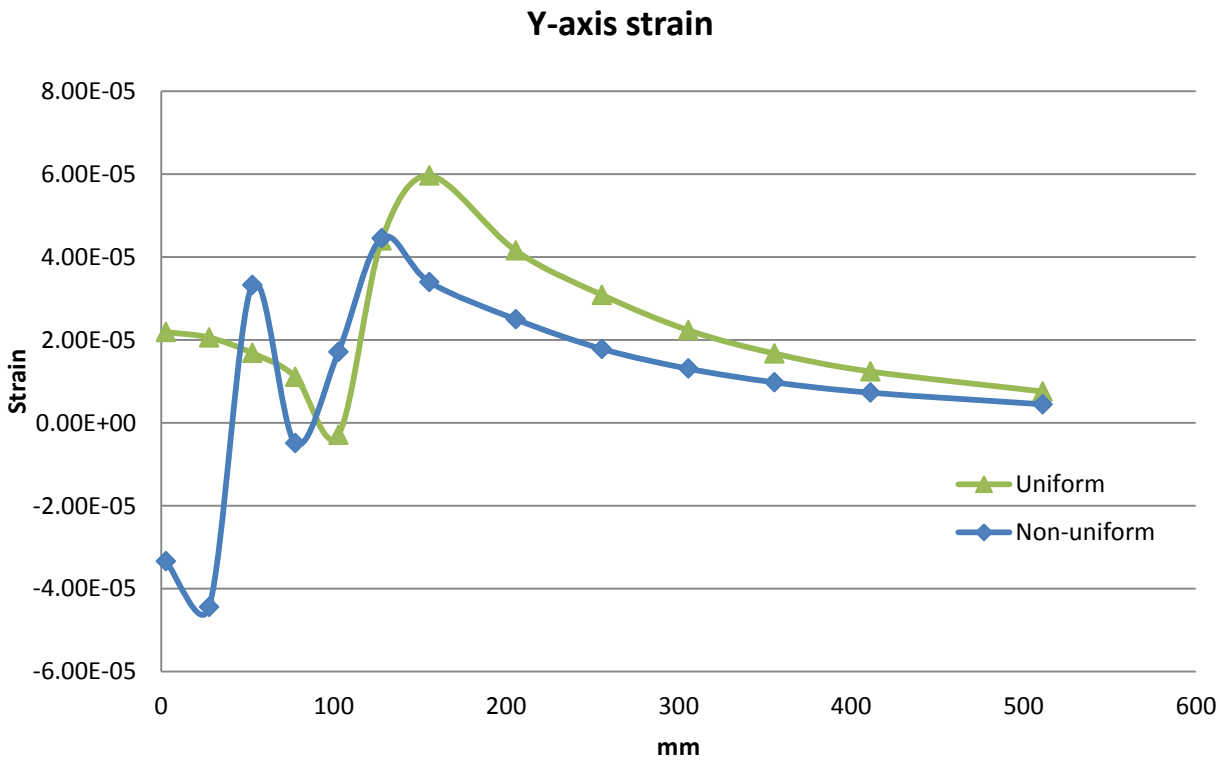
Y-axis strain
8.00E-05
6.00E-05
4.00E-05
2.00E-05
0.00E+00
-2.00E-05
-4.00E-05
-6.00E-05
Strain
0
100
200
300
400
500
600
mm
Uniform
Non-uniform

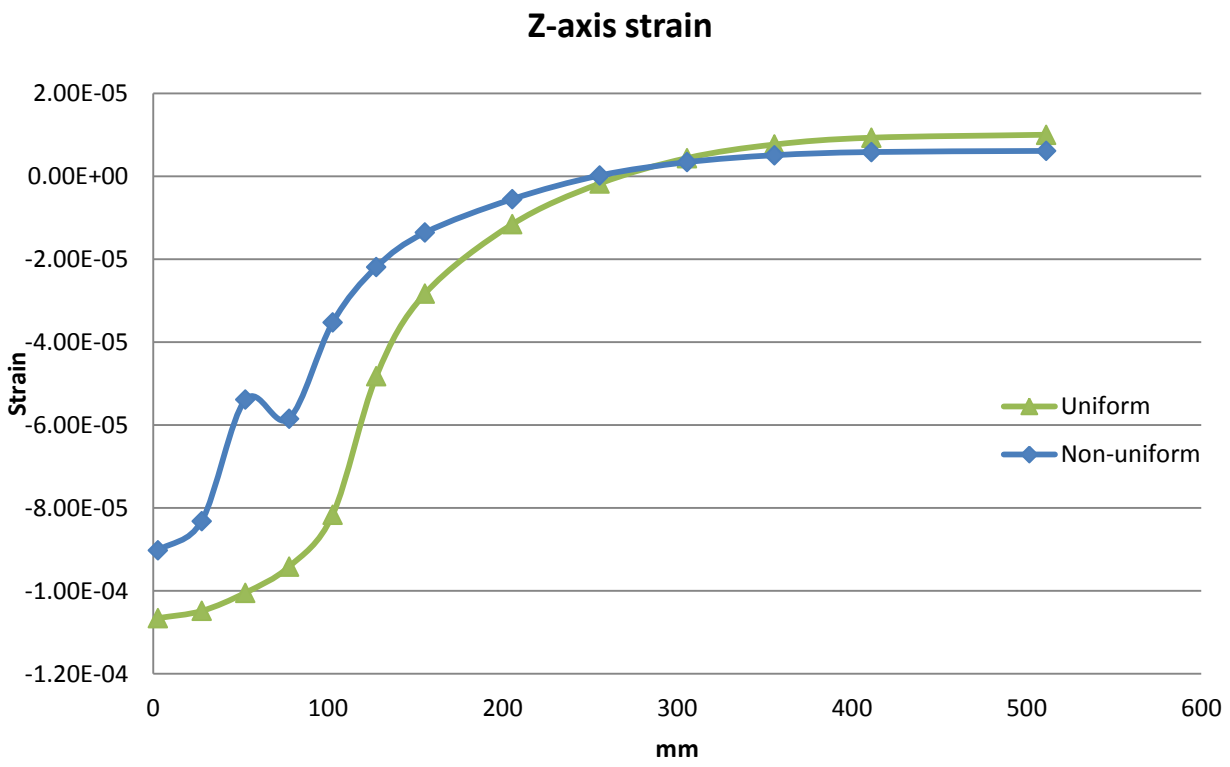

Figure 4 – Principal Strains for 2.5mm depths

It can be seen from the graphs in Figure 4 that the nature of the strains developed by the uniform and non-uniform pressure is completely different. The strains for the uniform contact stay constant over the majority of the loaded area. On the other hand, the non-uniform pressure generated strains vary widely across the loading area and only settles down outside the area of loading like the uniform pressure especially for the Y-axis strains. The largest variation can be seen in the Y strain component. The non-uniform contact pressure strain also reaches a peak under the contact area and is much larger than for the uniform contact pressure strains under the loaded area for the Y component. The strain also changes sign under the contact between the peak and the next point. However, the X and Z strain components for the uniform pressure are higher than for the non-uniform pressure. The difference for these components though is not as stark as for the Y component. There is little variation in either the uniform or non-uniform strains and they generally follow the same shape. It can be observed that the strain away from the contact area either reaches zero or tends towards it.

3.2 27.5MM DEEP PRINCIPAL STRAINS

The graphs presented in Figure 5 illustrate the principal strains that are observed for the two load cases at a depth of 27.5mm from the surface of the pavement. They show how the nature of the strain profiles changes with depth.

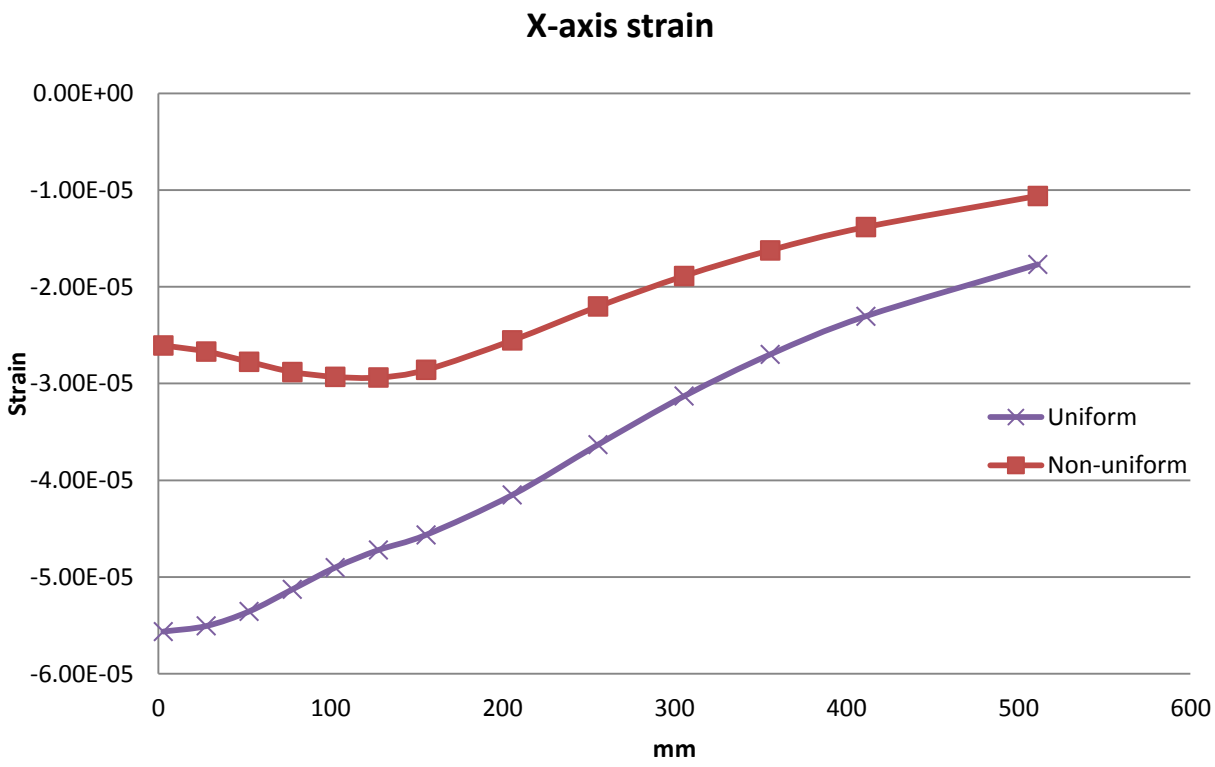
X-axis strain
0.00E+00
-1.00E-05
-2.00E-05
-3.00E-05
-4.00E-05
-5.00E-05
-6.00E-05
Strain
0
100
200
300
400
500
600
mm
Uniform
Non-uniform

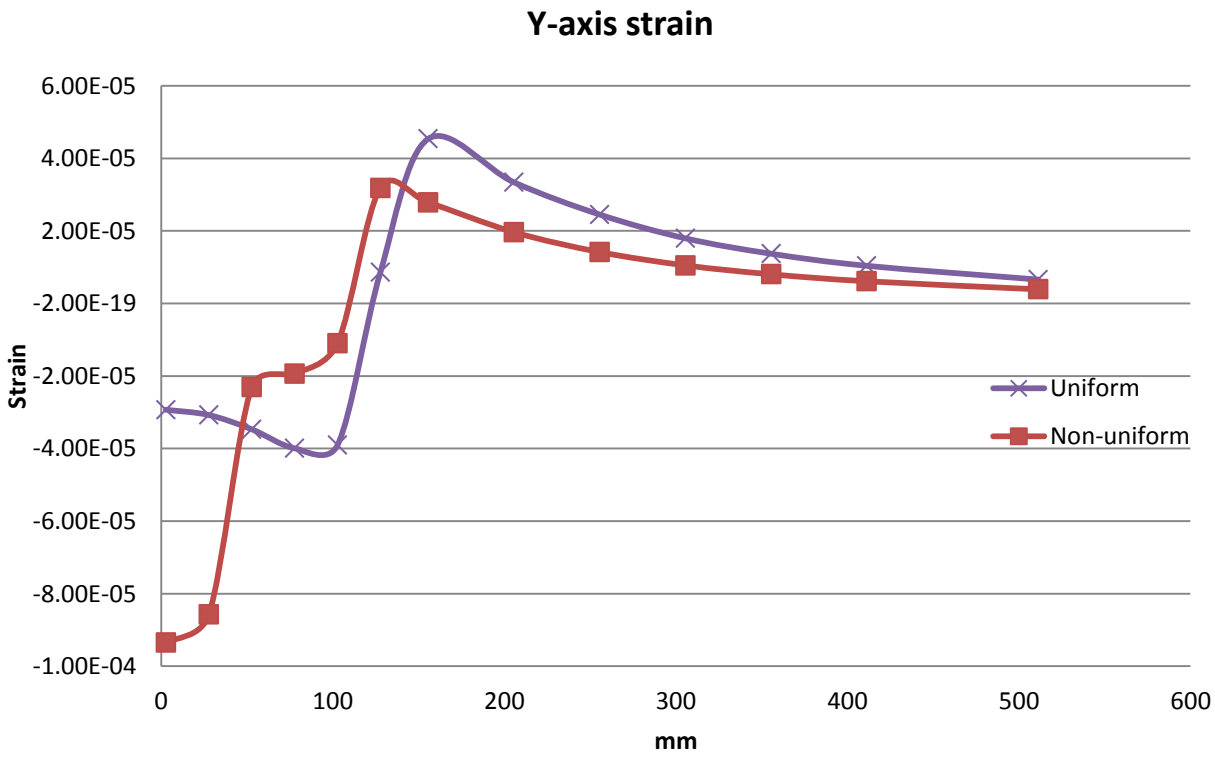
Y-axis strain
6.00E-05
4.00E-05
2.00E-05
-2.00E-19
-2.00E-05
-4.00E-05
-6.00E-05
-8.00E-05
-1.00E-04
Strain
0
100
200
300
400
500
600
mm
Uniform
Non-uniform

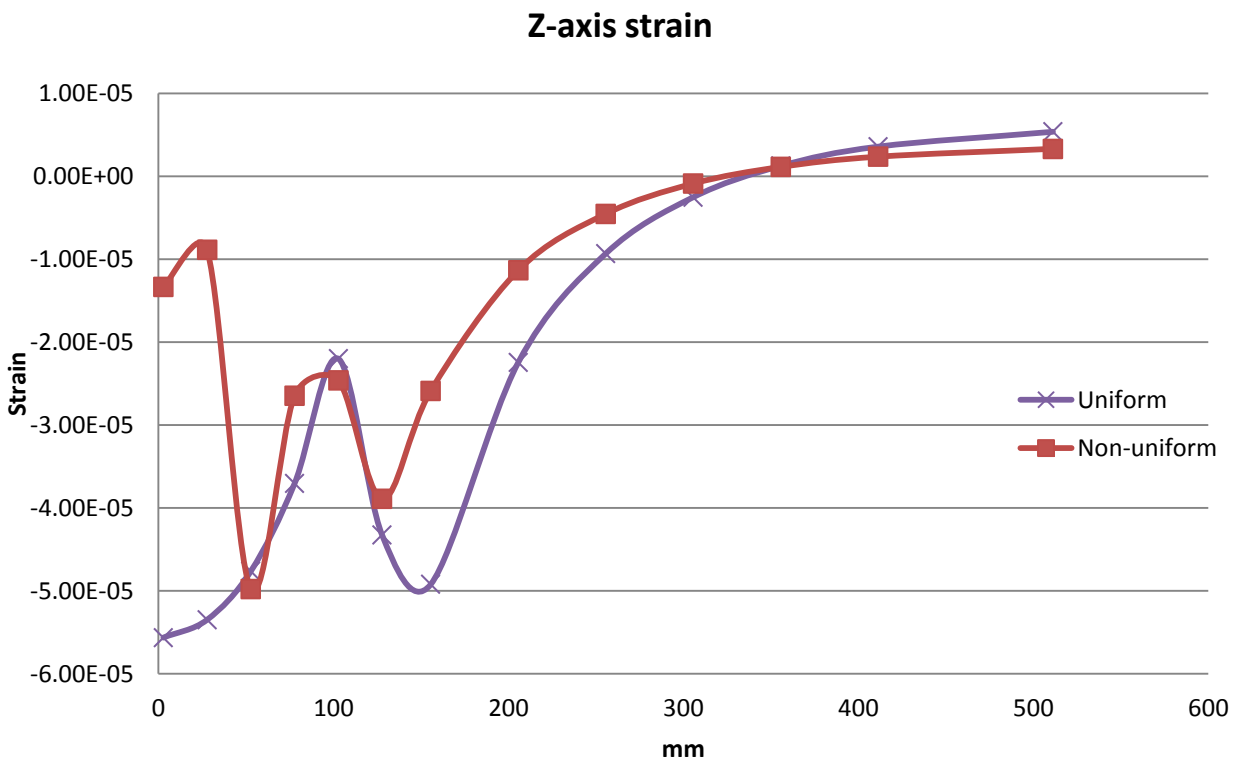

Figure 5 - Principal Strains for 27.5mm depth

It can be seen from the graph that the strain profile for the Y component of strain for the non-uniform loading remains high. The maximum reached is higher than in the 2.5mm graph. The peak strain is 93 microstrain in this component and it is also the overall maximum. This compares to a maximum for the uniform loading for this component of 39 microstrain.

The Y component of strain increased from the 2.5mm depth to the 27.5mm depth; however the other two components decreased. The strain profile has also diverged more for the uniform and non-uniform contact pressure in these two components of strain especially under the contact area. These two components do not have such a high peak value like the Y component. The X component has a peak of 55 microstrain for the uniform loading and 30 for the non-uniform loading. The Y component has a peak of 56 microstrain for the uniform loading and 50 microstrain for the non-uniform contact pressure. The strain illustrated for the Z and X components although higher for the uniform contact pressure is of a more marginal nature than for the Y component of strain.

3.2 LARGEST SHEARING COMPONENT AT 2.5MM DEPTH

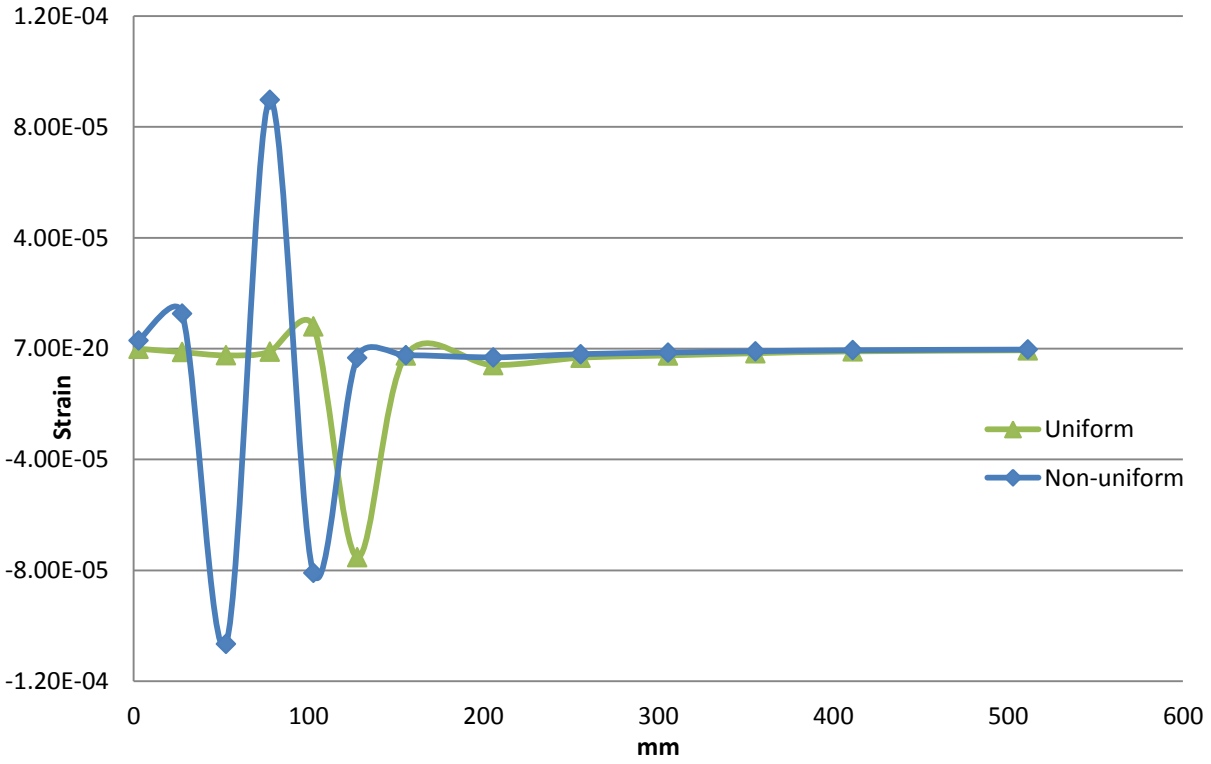

Figure 6 - YZ Strain Component at 2.5mm Depth

The graph in Figure 6 clearly illustrates the non-uniform shearing forces that are created by the non-uniform contact pressure. The shearing is quite high under the contact area and varies widely from -107 microstrain to 90 microstrain which are located side by side. This is a large swing and is in stark contrast to the uniform contact pressure which only exhibits a meaningful shear force at the edge of the contact area of -75 microstrain. This is the most striking difference between the two loading scenarios. This gives rise to a completely different strain state under the loading area. It gives rise to more distress in conjunction with the appropriate material and environmental factors. This generation of shear will be more pronounced with more detailed contact pressure geometries. This graph (Fig. 6) serves to illustrate the large strains that can be created with these simple contact pressure geometries. The strain levels for both loading scenarios from about 160mm from the centre of the loading display practically Zero strain showing that it is localised to the loading and near loading area.

4. CONCLUSIONS

The graphs presented in the Results and Discussion section provides the information to draw the following conclusions from this study on the near surface strain of uniform and non-uniform contact pressures.

- The peak strain levels are recorded for the non-uniform contact pressure for the principal axes for both the 2.5mm depth and the 27.5mm depth.
- The non-uniform contact pressure creates significant non-uniformity of strain under the contact area for the principal axis at both depths.

- Non-uniform contact pressure creates a largely varying shearing strain under the contact area. This is completely different than the uniform contact pressure case and not accounted for in current design procedure. The maximum of this strain is comparable in magnitude to the maximum principal axes strain.
- A highly complex strain state is created under the contact area of the non-uniform contact case in comparison to uniform contact pressure.

Overall, the non-uniform contact pressure distribution leads to a very different set of strain profiles for the principal axes and major shear component. This gives rise to a much different strain state under the contact area that will contribute to a different distress process which is currently not predicted with uniform contact pressure. The large shear strain created is of particular concern as it is in complete contrast to the uniform contact pressure case. This study gives a good insight into the behaviour of the near surface of the pavement for non-uniform contact pressure distribution in comparison to the uniform circular contact pressures currently employed in pavement analysis.

REFERENCES

1. American Association of State Highway & Transportation Office (1981) AASHTO interim guide for design of pavement structures, 1972, chapter III revised.
2. Greene J, Toros U, Kim S, Byron T, & Choubane B (2010) Impact of Wide-Base Single Tires on Pavement Damage. Transportation Research Record (2155):82-90.
3. Morton BS, Luttig E, Horak E, & Visser AT (2004) The Effects of Axle Load Spectra and Tyre Inflation Pressures on Standard Pavement Design Methods. 8th Conference on Asphalt Pavements for Southern Africa (CAPSA'04).
4. Wang F and Machemehl RB, Southwest Region University Transportation C, University of Texas at Austin. Center for Transportation R, & University Transportation Centers P (2006) Predicting truck tire pressure effects upon pavement performance (Southwest Region University Transportation Center, Center for Transportation Research, University of Texas at Austin, Austin, Tex.).
5. De Beer M, Fisher C., & Jooste F. J (1997) Determination of pneumatic tyre/pavement interface contact stresses under moving loads and some effects on pavements with thin asphalt surfacing layers. Eight (8th) International Conference on Asphalt Pavements (8th ICAP '97), pp 179-227.
6. Blab R (1999) Introducing Improved Loading Assumptions into Analytical Pavement Models Based on Measured Contact Stresses of Tires. International Conference on Accelerated Pavement Testing (Reno, NV).
7. Fernando EG, Musani D, Park D-W, & Liu W (2006) Evalution of Effects of Tire Size and Inflation Pressure on Tire Contact Stresses and Pavement Response. Technical Report, Texas Transportation Institute, Texas A&M University System College Station, Texas p 288.
8. De Beer M, Fisher, C and Kannemeyer (2004) Tyre-pavement interface contact stresses on flexible pavements – quo vadis? 8th Conference on Asphalt Pavements for Southern Africa (CAPSA'04), pp pages 1-22.
9. Uhlmeyer JS, Willoughby K, Pierce LM, & Mahoney JP (2000) Top-Down Cracking in Washington State Asphalt Concrete Wearing Courses. Transportation research record. (1730):110.
10. Jacobs MMJ, Hopman PC, & Molenaar AAA (1995) The crack growth mechanism in asphaltic mixes. Heron-English Edition- 40(3):181-200, Thesis.
11. Matsuno S & Nishizawa T (1992) Mechanism of Longitudinal Surface Cracking in Asphalt Pavement. in Proceedings of the 7th International Conference on Asphalt Pavements (Nottingham), pp. 277-291.
12. Baladi GY, Schorsch MR, & Svasdisant T (2003) Determining the causes of top-down cracks in bituminous pavements, Technical Report, (Michigan Dept. of Transportation, Construction & Technology Division, Testing and Research Section, Lansing, MI).
13. Novak M, Birgisson B, & Roque R (2003) Tire contact stresses and their effects on instability rutting of asphalt mixture pavements - Three-dimensional finite element analysis. Pavement Management and Rigid and Flexible Pavement Design 2003 (1853):150-156.
14. Perret J (2003) The effect of loading conditions on pavement responses calculated using a linear-elastic model, EPFL repository.